Article

Measurement of the Binding of Cholera Toxin to GM1 Gangliosides on Solid Supported Lipid Bilayer Vesicles and Inhibition by Europium (III) Chloride

Thomas L. Williams, and A. Toby A. Jenkins

J. Am. Chem. Soc., **2008**, 130 (20), 6438-6443 • DOI: 10.1021/ja710543x • Publication Date (Web): 16 April 2008

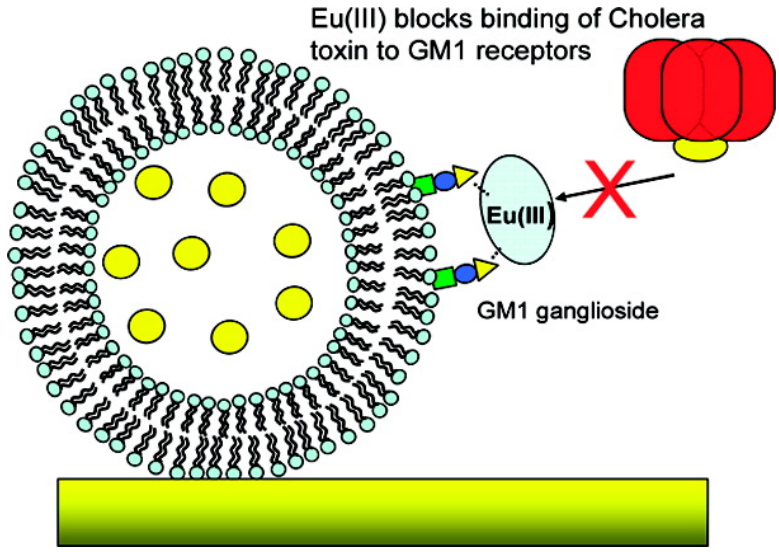

More About This Article

Additional resources and features associated with this article are available within the HTML version:

- Supporting Information
- Access to high resolution figures
- Links to articles and content related to this article
- Copyright permission to reproduce figures and/or text from this article

View the Full Text HTML

J|A|C|S
ARTICLES

Published on Web 04/16/2008

Measurement of the Binding of Cholera Toxin to GM1 Gangliosides on Solid Supported Lipid Bilayer Vesicles and Inhibition by Europium (III) Chloride

Thomas L. Williams and A. Toby A. Jenkins*

Department of Chemistry, University of Bath, Bath, BA2 7AY, United Kingdom

Received November 22, 2007; E-mail: a.t.a.jenkins@bath.ac.uk

Abstract: In this paper the immobilization of small unilamellar DMPC/GM1 lipid vesicles containing a water-soluble bodipy dye is described. The binding of the complete $\alpha\beta$ toxin expressed by *Vibrio cholerae* to the attached vesicles was measured using Surface Plasmon Resonance (SPR) and a value of the dissociation constant K_D obtained. Further measurements showed that the interaction of both the $\alpha\beta$-toxin and the β-subunit alone resulted in the permeation of the lipid membrane, with release of a fluorophore contained within the vesicle being measured by combined SPR and Surface Plasmon enhanced Fluorescence Spectroscopy (SPFS). The leakage of dye through the membrane, measured by following the change in fluorescence, was fitted to a simple diffusion model. Finally, SPFS measurements of the effect of europium(III) chloride ($EuCl_3$) showed that cholera toxin binding and subsequent membrane permeation could be blocked by 1 μmol dm^{-3} europium chloride. In view of the low oral toxicity of europium chloride, we speculate on the potential pharmaceutical applications of this molecule in the treatment of cholera infection.

Introduction

Cholera is a disease caused by the cholera toxin (*Ctx*) excreted by the bacterial pathogen *Vibrio cholerae* following infection and colonization of the mammalian gut. The toxin binds to epithelial cells in the gut causing massive electrolyte loss, expressed usually as watery diarrhea and vomiting, this leading to the classic dehydration associated with the disease. In severe cases, and with improper treatment, the disease can lead to acute renal failure, electrolyte imbalance, and even death.[1] Recent reports by The World Health Organization have shown a sharp rise in the number of cases of cholera in 2005, with around 130 000 cases, including 2272 deaths from 52 countries. This showed a 30% increase compared to figures in 2004.[2] This is why cholera is still a modern day problem and attracts attention from research groups around the world.

The cholera toxin binds to the GM1 ganglioside present on the surface of mammalian cells. The GM1, like many other glycolipids, is involved in cell adhesion, differentiation, apoptosis, and communication. However, bacterial cell membranes do not possess this class of cell surface receptors. Therefore, many microbial species have developed GM1-binding toxins as primary virulence factors. GM1 has long been known as the principal target receptor for the organisms *Vibrio cholerae*, *Salmonella typhimurium*, and *Escherichia coli*.[3] It is believed that one pentameric β-subunit binds up to five GM1 receptor sugars in the membrane.[4] The nature of the GM1−*Ctx* interaction has been studied in detail by Turnball et al. using Isothermal Titration Calorimetry (ITC), which allowed the key thermodynamic parameters to be obtained.[5]

The cholera enterotoxin (*Ctx*) expressed by *Vibrio cholerae* belongs to the $\alpha\beta_5$ family of toxins, possessing five identical β-subunit peptides forming a pentameric ring that binds up to five GM1 gangliosides on intestinal epithelial cells. The α-subunit associates with the β-pentamer, with the whole toxin internalized via endocytosis following binding to epithelial cell outer membranes.[6] The intracellular target of *Ctx* is the regulatory enzyme, adenylate cyclase, which modulates ATP to cyclic AMP. Disruption of the balance of adenylate cyclase results in increased protein phosphylation and alteration in ion transport, which ultimately expresses itself as the characteristic symptoms associated with cholera.[7]

Cholera toxin has been widely studied, with a range of methodologies employed to follow the mode of action of the toxin, including in vivo whole animal studies, erythrocyte ghosts, and model membranes.[8,9] The complexity of the action of bacterial infection means that, in complex systems, such as a whole animal, it can be difficult to precisely elucidate the mode of action of bacteria and associated toxins. As a consequence, model systems have been developed containing artificial biomimetic epithelial membranes to study the specific recognition and binding of *Ctx* and the GM1 ganglioside present on cell

(1) Sack, D. A.; et al. *Cholera. Lancet* **2004**, *363*, 223–233.
(2) WHO, *Weekly epidemiological record.* World Health Organization: 2006; Vol. 81, pp 297−308.
(3) Kuziemko, G. M.; Stroh, M; Stevens, R. C. *Biochemistry* **1996**, *35*, 6375–6384.
(4) Lencer, W. I. *Am. J. Physiol. Gastrointest. Liver Physiol.* **2001**, *280*, G781–G786.
(5) Turnbull, W. B.; Precious, B. L.; Homans, S. W. *J. Am. Chem. Soc.* **2004**, *126*, 1047–1054.
(6) Lencer, W. I.; Tsai, B. *Biochem. Sci.* **2003**, *28*, 639–645.
(7) Kaper, J. B.; Morris, G; Levine, M. M. *Clin. Microbiol. Rev.* **1995**, *8*, 316–316.
(8) Schiavo, G.; van der Goot, F. G. *Nat. Rev. Mol. Cell Biol.* **2001**, *2*, 530–537.
(9) Ikigai, H.; Akatsuka, A.; Tsujiyama, H.; Nakae, T.; Shimamura, T. *Infect. Immun.* **1996**, *64*, 2968–2973.

10.1021/ja710543x CCC: $40.75

surfaces. Early work in this area on solid supported lipid membranes used simultaneous Surface Plasmon Resonance (SPR) and electrochemical impedance, to follow the binding of the *Ctx* β-subunit.[10] More recently, Edwards and March developed a sensing strategy based on GM1 containing vesicles with an encapsulated, self-quenching fluorescent dye contained within a microtiter plate. Cholera toxin, if present, bound to a plate immobilized antibody, with the GM1 vesicles binding to the cholera. Surfactant induced lysis of the bound vesicles optimized (lowered) the Limit of Detection (LoD) compared to classical antibody assays.[11]

In this work, an artificial membrane consisting of whole lipid vesicles of diameter ca. 100 nm were attached to a matrix of the tetrameric protein streptavidin, itself attached to a biotinylated labeled Self-assembled Monolayer (SAM). This methodology is a modification of our previous approach detailed in our former publication; it utilizes a structured, biotinylated Self-assembled Monolayer (SAM) and streptavidin for surface attachment of the biotin tagged vesicles and follows on from the work of Boukobza et al.[12,13] Although it is not the most sophisticated of vesicle support systems detailed in the literature, it has the virtues of ease of fabrication and reproducibility of vesicle attachment. One disadvantage is a relatively high passive leakage, probably as a result of vesicle "pinning", which can be reduced by use of "softer" support structures such as polymers. However, these surfaces can be more complex to fabricate and are not as reproducible.[14] Europium has recently been shown to be an effective way of labeling GM1 sugars for fluorescence studies.[15] We show that the presence of europium bound to the GM1 receptor effectively blocks the binding of the $\alpha\beta$ cholera toxin. The fluorescent properties of the europium are not probed in this study.

Experimental Section

Formation of Supported Vesicles on Surface. Thin gold films (ca. 50 nm thick) were made by thermal evaporation of gold in an Emitech K975 thermal evaporator onto high refractive index (n = 1.80) $LaSFN_9$ glass slides (Berliner glass) at a pressure of 4×10^{-6} mb. The coated glass was subsequently annealed at 450 °C for 2 min and then cleaned under a high intensity UV lamp/ozone for 10 min before rinsing in ethanol. A binary SAM consisting of a biotin thiol and mercaptounadecaol lateral spacer was formed by immersion of the clean gold/glass slides in an ethanolic solution of the two thiol moieties at 1 mol % 11-mercaptododecanoic-(8-biotinoyl-amido-,3,6-dioxaoctyly) amide (thiol−biotin) and 99% mercaptoundecanol (Sigma) for 16 h before rinsing in ethanol and water. The biotin thiol consists of a C11 mercapto-alkyl chain, three ethoxy spacer units, and a biotin headgroup.[16] The thiol biotin was synthesized in our laboratory following the procedure described by Booth et al.[17] The biotin surface was coupled to streptavidin (500 nmol dm^{-3} in 10 mmol dm^{-3} HEPES buffer containing 2 mmol dm^{-3} $CaCl_2$ and 150 mmol dm^{-3} NaCl, to create the "capture" surface for the lipid vesicles.

Small unilamellar lipid vesicles were made by mixing 67 mol % dimyristolyl-phophatidylcholine (DMPC), 30 mol % cholesterol, 2 mol % GM1, and 1 mol % dipalmitoyl-phosphoethanol-amine-*N*-biotinyl (DPPE-biotin) (Sigma U.K.) in chloroform and drying under vacuum for 12 h and resuspending in the HEPES/$CaCl_2$/NaCl buffer described above, with 1 μmol dm^{-3} water soluble bodipy dye (6-(((4,4-difluoro-5-(2-pyrrolyl)-4-bora-3a,4a-diaza-s-indacene-3-yl)styryloxy)acetyl) aminohexanoic acid, sulfotetrafluorophenyl ester, sodium salt, Invitrogen) (ex_{max} = 648 nm, em_{max} = 660 nm) added to give a final lipid concentration of 0.4 mg mL^{-1}. The lipid suspension was extruded through 100 nm diameter pores in a polycarbonate membrane in a lipid extruder (Avestin). The biotin tagged vesicles were added to the streptavidin catcher surface, and binding followed using Surface Plasmon Resonance. Vesicles were allowed to bind for 30 min before rinsing in buffer to remove the nonencapsulated fluorophore and nonbound vesicles from the system. Whole *Ctx* and β-subunit of *Ctx* were both obtained from Sigma U.K. Whole *Ctx* should be used with care and not internalized.

Surface Plasmon Resonance(SPR) and Surface Plasmon Enhanced Fluorescence (SPFS) Measurements. SPR was used to follow the construction of the modified surface. Full details of the SPR/SPFS system are provided in refs 18 and 19. SPR measures the angle of resonance when light is coupled into a thin metal film, normally via a prism. The angle at which surface plasmon resonance takes place, observed as a reflection minimum, is highly sensitive to changes in the dielectric constant. The adsorption or loss of a surface film on a metal surface within the evanescent field can thus be measured *in situ* and in real time. The home-built instrument used in these experiments followed the changes in reflection intensity at an angle around 1.5° lower than the resonance angle. Hence, changes in reflected light intensity at the fixed angle allowed real-time measurement of toxin binding.

Modeling of Dye Flux through Vesicles. In order to more accurately quantify the effect of toxin binding to the vesicles, a simple theoretical model was developed to fit the decrease in fluorescence−time curves obtained following toxin interaction. A simple model is to assume that all vesicles are of a uniform size with a total internal volume V, and a total area A and membrane thickness d. Concentration of fluorescent dye within vesicles is C_{in}. A straightforward diffusion model based on Fick's first law, for the diffusion flux, J of dye through the membrane is given by

$$J = \frac{KDc_{in}}{d} \tag{1}$$

where K relates to the partitioning of dye into the membrane, $K = C_{mem}/C_{in}$, and D is the diffusion coefficient of the dye through the membrane. The change in internal concentration of dye with time can thus be approximated:

$$\frac{dC_{in}}{dt} = \frac{AJ}{V} = \frac{AKDC_{in}}{Vd} \tag{2}$$

This is a first order kinetics equation, which can be further simplified and integrated to give eq 3:

$$\ln C_{in} = \ln C_{in,o} - kt \tag{3}$$

where k is the first order rate constant

$$k = \frac{AKD}{Vd} \tag{4}$$

The term A is the internal surface area of the vesicle, V, the volume of a vesicle, and d, the membrane thickness. This gives

(10) Terrettaz, S.; Stora, T.; Duschol, C.; Vogel, H. *Langmuir* **1993**, *9*, 1361–1369.
(11) Edwards, K. A.; March, J. C. *Anal. Biochem.* **2007**, *368*, 39–48.
(12) Williams, T. L.; Vareiro, M. M. L. M.; Jenkins, A. T. A. *Langmuir* **2006**, *22*, 6473–6476.
(13) Boukobza, E.; Sonnenfeld, A.; Haran, G. *J. Phys. Chem. B* **2001**, *105*, 12165–12170.
(14) Chifen, A.; Foerch, R.; Knoll, W.; Khor, H.; Cameron, P. J.; Williams, T. L.; Jenkins, A. T. A. *Langmuir* **2007**, *23*, 6294–6298.
(15) Alptürk, O.; Rusin, O.; Fakayode, S. O.; Wang, W.; Escobedo, J. O.; Warner, I. M.; Crowe, W. E.; Král, V.; Pruet, J. M.; Strong, R. M. *Proc. Natl. Acad. Sci. U.S.A.* **2006**, *103*, 9756–9760.
(16) Vareiro, M. L. M. M.; Liu, J.; Knoll, W.; Zak, K.; Williams, D.; Jenkins, A. T. A. *Anal. Chem.* **2005**, *77*, 2426–2431.
(17) Booth, C.; Bushby, R. J.; Cheng, Y.; Evans, S. D.; Liu, Q.; Zhang, H. *Tetrahedron* **2001**, *57*, 9859–9866.
(18) Yu, F.; Persson, B.; Löfäs, S.; Knoll, W. *J. Am. Chem. Soc.* **2004**, *126*, 8902–8903.
(19) Liebermann, T.; Knoll, W. *Langmuir* **2003**, *19*, 1567–1572.

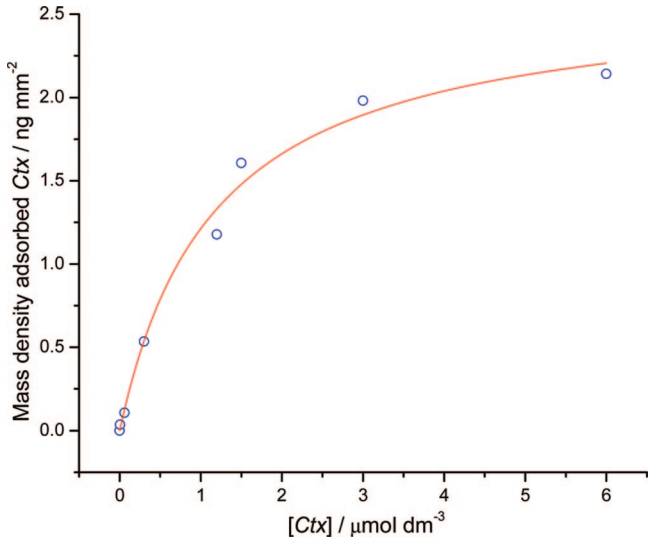

Figure 1. Plot of change in mass density of bound *Ctx* measured by SPR vs solution concentration of *Ctx*. The Langmuir eq 5 was fitted to the data to allow determination of K_D.

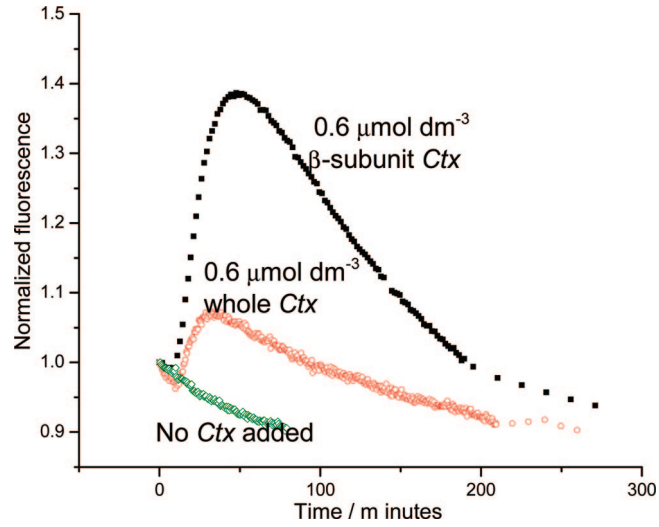

Figure 2. SPFS measurement of change in fluorescence of surface immobilized vesicles on addition of whole *Ctx* and β-subunit *Ctx*. The passive leakage of dye from vesicles not exposed to toxin is also shown.

dimensionally correct units of rate constant k in s^{-1}. Since the membrane partition coefficient K is not known, the term D^* termed the apparent diffusion coefficient is the sum of KD ($D^* = KD$). Hence, dye leakage, measured as a decrease in fluorescence, was fitted to eq 3, in order to quantify dye leakage as a result of *Ctx*−vesicle interaction and the relative efficiency of binding inhibitors. As the external volume is many times larger than the internal volume of vesicles (ca. 0.5 mL) and that the fluorophore experiences enhanced fluorescence only within a ca. 200 nm zone close to the gold slide, the assumption was made that the effective concentration of dye outside of the vesicles was zero.

Results and Discussion

Interaction of Cholera Toxin with Lipids Vesicles. Initial experiments on the tethered vesicles used SPR to quantify the vesicle membrane−*Ctx* equilibrium dissociation constant K_D. The equilibrium binding response after adding *Ctx*, measured as the mass density of bound m_{Ctx} (proportional to the change in reflection minimum at $\theta_{resonance}$), was plotted against the solution concentration of toxin in solution, [*Ctx*] (Figure 1), using the empirical relationship developed by Yu et al. and used in previous studies of protein binding.[19,17] K_D was determined directly from the plot by fitting the data to the Langmuir binding isotherm:

$$m_{Ctx} = \frac{m_{max}[Ctx]}{K_D + [Ctx]} \quad (5)$$

The calculated K_D for the interaction between the vesicles and cholera toxin was $(1.16 \pm 0.2) \times 10^{-6}$ mol dm^{-3}, which was in broad agreement with other reported K_D values for this interaction.[20] It should be noted that measurements of the strength of this interaction appear very dependent on the measurement methodology and experimental setup, with K_D varying between 3×10^{-8} mol dm^{-3} (SPR by Terrettaz et al. on planar lipid membranes [11]) to as high as 2.2×10^{-5} mol dm^{-3}(quasi dynamic light scattering on *Ctx* mediated agglutination of GM1 modified vesicles and polystyrene spheres by Dwyer and Bloomfield [21]). Measurements of nonspecific toxin binding to the surface were also made using GM1 deficient vesicles. A K_D 2 orders of magnitude larger was obtained, illustrating the specificity of the GM1 receptor in toxin binding.

Surface Plasmon Enhanced Fluorescence Measurement of *Ctx*− and *Ctx* β-Subunit−Vesicle Interaction. The next part of the study looked at the change in fluorescence as surface tethered vesicles containing fluorophores interacted with both whole *Ctx* and β-subunit *Ctx*. The change in fluorescence with time plot for both systems is shown in Figure 2. The response was unexpected, with an initial increase in fluorescence, followed by a decrease, but found to be highly reproducible and quite unlike previous measurements with phopholipase A_2, where rapid dye leakage was observed.[13] Figure 2 suggests that the interaction of *Ctx* with the vesicle induces a significant change in the measured fluorescence on the surface immobilized vesicles. The addition of *Ctx* appears to enhance the measured fluorescence for a considerable time, with the enhancement effect being greater for the β-subunit of *Ctx* than the whole *Ctx*. The initial enhancement observed on the surface immobilized vesicles subsequently decreases, presumably as a consequence of increased dye permeability of the membrane following toxin addition. Over longer time periods, loss in fluorescence was measured, attributed to *Ctx* mediated permeation of the bilayer.

The nature of the interaction of the β-subunit (which binds to the GM1 receptor) with the membrane is not fully characterized. Miller et al. in 1995 used neutron scattering and Monte Carlo simulation to study the interaction of the β-subunit of the cholera toxin with lipid monolayers at the air−water interface. They concluded that the β-subunit itself does not penetrate the lipid membrane, but geometrical constraints on lipid packing caused by the toxin−multi-GM1 interaction led to a decrease in lipid packing density.[22] Other researchers claim that the *Ctx* forms a pore on the noncovalent binding of the β-subunit to GM1 receptor sugars on the cell surface, with a

(20) Lauer, S.; Goldstein, B.; Nolan, R. L.; Nolan, J. P. *Biochemistry* **2002**, *41*, 1742–1751.

(21) Dwyer, J. D.; Bloomfield, V. A. *Biochemistry* **1982**, *21*, 3231–3234.

(22) Miller, C. E.; Majewski, J.; Faller, R.; Satija, S.; Kuhl, T. L. *Biophys. J.* **2004**, *86*, 3700–3708.

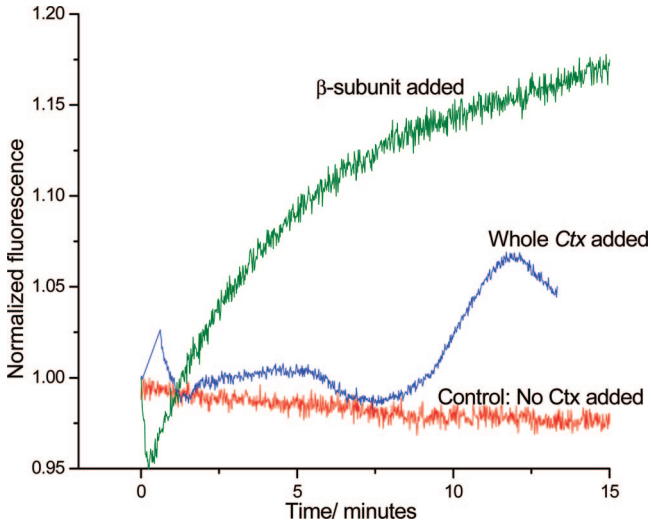

Figure 3. Fluorescence measurements (using 633 nm laser excitation) of nonimmobilized vesicles on addition of *Ctx* and β-subunit *Ctx*.

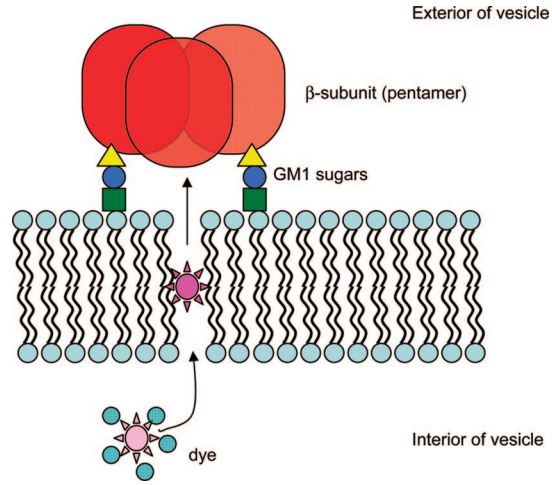

Figure 4. Schematic of proposed mechanism of fluorescent enhancement on binding of *Ctx* to GM1 modified lipid. Fluorescent dye, partially quenched by solvent−water, is dequenched in lipid membrane made leaky by attachment of the β-subunit of *Ctx* to GM1 receptors on the membrane surface. To aid clarity, the α-subunit is not drawn.

diameter between 11 and 15 Å, although the extent to which this pore penetrates the membrane is still unclear.[23]

The interpretation of Figure 2 focused on two possible mechanisms: (1) Was *Ctx* causing a conformational change in the adsorbed vesicles resulting in a flattening ("pancaking") of the vesicles, resulting in a greater proportion of dye experiencing a stronger enhancement from surface plasmon resonance? (2) Was the dye interacting with the β-subunit on or in the membrane, perhaps as a result of pore formation/membrane disruption by the β-subunit? In order to try to eliminate the former possibility, experiments were performed using the SPFS instrumentation, but with a quartz cuvette in place of the conventional prism/gold and the PMT detector placed at 90° to the incident 633 nm laser, in effect making a conventional fluorimeter. The further possibility that the dye was being self-quenched in the vesicle and release of dye on *Ctx* binding resulted in reduced self-quenching was discounted by making careful fluorometric studies of the dye at a range of concentrations. There was no evidence of self-quenching in or close to the concentration range used in the experiment. Concentrations of toxins were identical to those used in experiments on surface tethered vesicles (Figure 2).

The results of the experiment are shown in Figure 3. It can be seen that both whole *Ctx* and β-subunit *Ctx* appeared to give an enhanced fluorescence response on interaction with vesicles, but with a much stronger effect being observed from the β-subunit *Ctx*. This result suggests that the β-subunit is actually forming a pore in the membrane through which the dye can diffuse through, since the whole *Ctx* is partially blocked by the presence of the α-subunit, resulting in lower permeability.

The consequence of the results in Figures 2 and 3 suggests that a possible mechanism for the enhanced response is not vesicle conformational change on the surface but some interaction of the encapsulated dye with the β-subunit. We speculate a channel of some kind, perhaps caused by the disordering of the lipid membrane structure proposed by Miller et al.[23] The increase in fluorescence could be caused by stripping of water from the dye as it interacts/passes through the "channel" resulting in partial dequenching. It must be pointed out that this is a working model and may not be correct, but it appears to fit the measured data. Moreover, it also accounts for the greater fluorescence enhancement observed when the β-subunit was used compared with whole *Ctx*, since the α-subunit may partially or completely impede passage of dye through the protein/membrane. A schematic picture of the model is shown in Figure 4.

Combined SPR and SPFS Measurements with/without GM1. As a further control measurement, combined SPR/SPFS measurements were made on vesicles in the absence of the GM1 receptor (Figure 5a). The SPR change on binding of *Ctx* and fluorescent change of vesicles containing GM1 are shown in Figure 5b for direct comparison.

Figure 5a shows that, in the absence of the GM1 receptor, a slow binding of toxin to the surface is observed, following an initial decrease in reflectance. The fluorescence shows an increase and behavior qualitatively similar to those of the system where the GM1 receptor is present in Figure 5b on adding toxin. The binding of the toxin in the absence of GM1 can potentially be explained by the role of the cholesterol in the membrane. Zitzer et al. have described the essential role of membrane cholesterol in the binding of two structurally different toxins, streptolysin O and *Vibrio cholerae* cytolysin.[24] These results suggest that cholesterol can also mediate the attachment of *Ctx* to membranes, although less effectively (in terms of binding) than when the GM1 receptor is also present. Figure 5b shows the effect of both cholesterol and the GM1 receptor in the membrane. Binding of the toxin is seen, measured by SPR and the effect on the vesicle fluorescence by the toxin, discussed earlier. The measurement of *Ctx* to vesicles deficient in both cholesterol and GM1 was attempted, but the very high passive leakiness of these vesicles made interpretation of the results very difficult.

Effect of Blocking *Ctx* Binding with Lanthanide III Salts. Having demonstrated that the effect of *Ctx* binding with vesicles could be observed using the combined SPR/SPFS methodology,

(23) Hirst, T. R.; D'Souza, J. M. In *The Comprehensive Sourcebook of Bacterial Protein Toxins*; Alouf, J. E., Popoff, M. R., Eds.; Elsevier: 2006; pp 270−284..

(24) Zitzer, A.; Westover, E. J.; Covey; D, F.; Palmer, M. *FEBS Lett.* **2003**, *553*, 229–231.

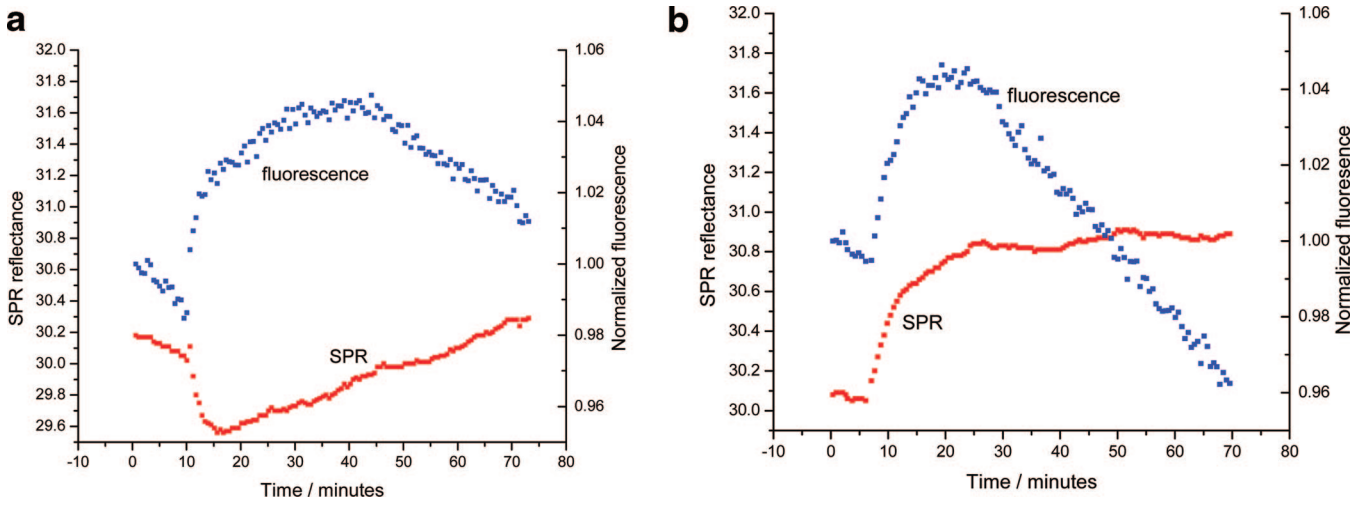

Figure 5. (a) SPR and SPFS response when vesicles without GM1 were immobilized (control experiment). It is hypothesized that this is a cholesterol mediated interaction. (b) SPR and SPFS experiment where 2 mol % GM1 was incorporated into vesicles.

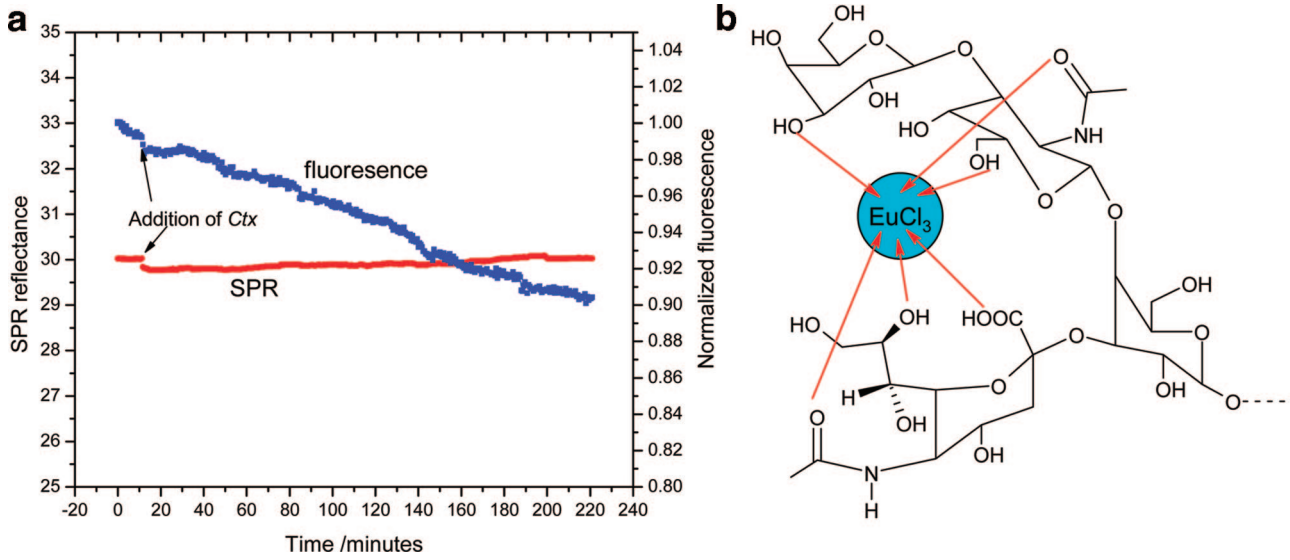

Figure 6. (a) Effect of adding 1 μmol dm^{-3} $EuCl_3$ to the vesicles prior to addition of 0.6 μmol dm^{-3}*Ctx*. The inhibition of the toxin binding and membrane permeation is seen. (b) Schematic of Eu(III) binding to GM1 and thus inhibiting binding of *Ctx*. Figure adapted from Alptürk et al.[15]

the next part of the study focused on inhibiting the binding of *Ctx* toxin to the membrane surface. A number of groups have studied the inhibition of *Ctx*−GM1 interaction with a view to developing drugs for relief of the symptoms of cholera infection. Monferran et al. used glycopeptides derived from pig gastric mucins to inhibit binding on erythrocyte ghosts.[25] The main focus of much current research (in 2007) is based on using oligomeric sugars for inhibition (by competitive binding to the *Ctx*−β-subunit).[26] Related work by Polizzotti et al. studied cholera toxin inhibition by glycopolymers with a polyglutamic acid based backbone.[27] McDaniel and McIntosh demonstrated in 1986 that the high affinity of GM1 in lipid vesicles for europium chloride did not change the hydrocarbon region of the bilayer; all changes in electron density following Eu(III) binding were seen in the phospholipid head region, but the bound Eu(III) does affect the extent to which the GM1 extends from the phospholipid lead group.[28] A separate article, published by Alptürk et al., demonstrated that a range of lanthanide III ions, including Eu(III), bind very strongly to sialic acid containing sugars including the GM1 ganglioside.[15] The application of the reported study was to use the fluorescent properties of the lanthanide ions as fluorescent markers for cancer (cancer cells tend to by highly glycosylated). It occurred to us that such ions may also block the binding of GM1 to *Ctx* since the strong multivalent interaction of the GM1 sugars−lanthanide III would likely have a higher binding constant than GM1−*Ctx*.

Ctx Inhibition by Eu(III). In this experiment, a 1 μmol dm^{-3} solution of europium(III) chloride (Eu(III)) was added to the surface immobilized vesicles containing 2 mol% GM1 (standard lipid composition). The europium salt was allowed to bind for 30 min. Following binding, 0.6 μmol dm^{-3} *Ctx* was added to

(25) Monferran, C. G.; Roth, G. A.; Cumar, F. A. *Infect. Immun.* **1990**, *58*, 3966–3972.
(26) Pukin, A. V.; Branderhorst, H. M.; Sisu, C.; Weijers, C. A. G. M.; Gilbert, M.; Liskamp, R. M. J.; Visser, G. M.; Zuilhof, H.; Pieter, R. J. *Chem. Biol. Chem.* **2007**, *8*, 1500–1503.
(27) Polizzotti, B. D.; Kiick, K. L *Biomacromolecules* **2006**, *7*, 483–490.
(28) McDaniel, R. V.; McIntosh, T. J. *Biophys. J.* **1986**, *49*, 94–96.

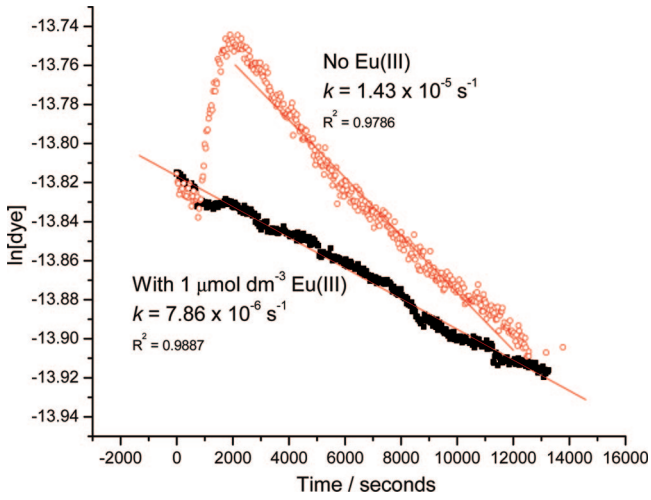

Figure 7. Plot of dye leakage data for vesicles following addition of 0.6 μmol dm^{-3} whole *Ctx* and waiting for any fluorescence increase to take place. Gradient from linear fit gives first order diffusion coefficient, used to determine the apparent diffusion constant of the dye through the membrane following toxin binding. Note the increase in dye concentration in measurement without Eu(III) is an apparent increase, due to the fluorescence change observed in Figure 5b, discussed above.

the vesicle and simultaneous SPR/SPFS measurements were made. The result was very different in the absence of the europium salt. The binding of the *Ctx* to the surface and the change in fluorescence seen in Figure 5b were not observed. The proposed binding of Eu(III) to the GM1 is schematically illustrated in Figure 6b.[16] Preincubation of the vesicles with Eu(III) was necessary to observe the inhibition shown in Figure 6a. Larger concentrations of Eu(III) were effective at blocking *Ctx* binding, but at concentrations below 1 μmol dm^{-3} the inhibition of toxin binding was lost: both binding of *Ctx* and increased dye permeation were both observed at concentrations of Eu(III) at 0.2 μmol dm^{-3} and below.

Stabilization of Vesicles to Passive Dye Diffusion by Eu(III) Ions. The effect of Eu(III) ions in preventing membrane permeation by the toxin was further confirmed by calculating the apparent dye diffusion coefficient upon addition of the *Ctx* to the membrane vesicles using the model detailed earlier. The fluorescent dye concentration was estimated from the measured fluorescence and plotted as a ln[dye] vs time graph from eq 3. This plot is shown in Figure 7, with linear fitting of data giving the first order rate constant k. Equation 4 was used to estimate the apparent dye diffusion coefficient D^* for the two systems, with a value of 6.5×10^{-22} m^2 s^{-1} for the system with Eu(III) inhibition and 1.3×10^{-21} m^2 s^{-1} without Eu(III) having been added. Thus it can be seen that *Ctx* increases the permeability of the membrane when Eu(III) was not present (following the initial fluorescence increase shown in Figure 2). This may be a consequence of the decrease in lipid packing density observed by Miller.[23] The slower diffusion of dye in the Eu(III) containing vesicles is attributed to passive diffusion (leakiness) of the dye through the vesicles, probably as a consequence of their being pinned to the support SAM by biotin-streptavidin. The rate of dye diffusion before adding toxin is the same as that after toxin addition, in the Eu(III) inhibited vesicles (Figure 7); in the noninhibited vesicles, diffusion is more rapid following toxin addition.

Conclusions

These results raise some important points. The first is that it appears that Eu(III) is an effective inhibitor of *Ctx* binding, at least in our model vesicle system discussed here. The mode of inhibition is based on the strong binding of Eu(III) to the GM1 sugars, which would otherwise bind the *Ctx*. One interesting implication of this work is that Eu(III) salts may be an effective drug following cholera infection. The reported toxicity (LD_{50}) of $EuCl_3$ is actually rather low (in rats) and reported to be 3527 mg kg^{1-} rat (oral),[29] compared with 3000 mg kg^{1-} rat (oral) for NaCl. The authors would be very interested to hear of results from the use of Eu(III) in this capacity, perhaps from *in vivo* studies.

The other interesting observation from these studies is the increase in membrane permeability to the fluorescent dye induced by *Ctx* binding. This effect may lead to a mechanism of secondary toxicity of *Ctx*. Although the primary, acute toxicity of *Ctx* is well established and, discussed earlier, if the increased permeability observed in this model system is also observed in cellular systems, or in whole organisms, then this could lead to an electrolyte imbalance and a further mechanism for cell death.

Acknowledgment. T.L.W. would like to thank the NERC for funding of his studentship. Thanks are also extended to Frank Marken (University of Bath) for assistance in developing the vesicle permeation model.

JA710543X

(29) Sigma-Aldrich MSDS sheet for $EuCl^3$.